

# Emergent patterns in a spin-orbit coupled spin-2 Bose-Einstein condensate

Z. F. Xu,<sup>1</sup> R. Lü,<sup>1</sup> and L. You<sup>1</sup>

<sup>1</sup>*Department of Physics, Tsinghua University, Beijing 100084, People's Republic of China*

(Dated: October 16, 2018)

The ground-state phases of a spin-orbit (SO) coupled atomic spin-2 Bose-Einstein condensate (BEC) are studied. Interesting density patterns spontaneously formed are widespread due to the competition between SO coupling and spin-dependent interactions like in a SO coupled spin-1 condensate. Unlike the case of spin-1 condensates, which are characterized by either ferromagnetic or polar phase in the absence of SO, spin-2 condensates can take a cyclic phase, where we find the patterns formed due to SO are square or triangular in their spin component densities for axial symmetric SO interaction. Both patterns are found to continuously evolve into striped forms with increased asymmetry of the SO coupling.

PACS numbers: 03.75.Mn, 03.75.Hh, 67.85.Fg

## I. INTRODUCTION

The technique of gauge field is a useful tool in theoretical physics. Depending on commutation relations of the associated operators, gauge fields are classified into Abelian and non-Abelian ones. An important example for Abelian gauge field concerns the well studied vector and scalar potentials of electromagnetic fields. Interesting phenomena, such as integer and fractional quantum hall effects are observed in two-dimensional high mobility electrons inside a perpendicular magnetic field. For a collection of cold atoms, Abelian gauge field can be affected through rotation [1, 2] or adiabatic motion inside far off-resonant laser fields [3–6]. While Abelian gauge fields are often studied, recent interests in Bose condensed atoms are increasingly targeted at situations when gauge fields become non-Abelian [3, 7–9]. One of the simplest examples concerns spin-orbit (SO) coupling, which recent understandings increasingly view as exists intrinsically in solid-state systems [10, 11], and is responsible for the quantum spin hall effect. In atomic quantum gases, SO coupling has been proposed with a variety of approaches involving atomic interactions with electromagnetic fields [3, 7, 12–18], including schemes for two component or pseudo spin-1/2 atomic condensates [14, 15] and spin-1 condensates [7, 13], and realized experimentally for pseudo spin-1/2 system recently [16].

Spin-orbit interaction couples the internal (spin) and orbital (momentum or angular momentum) degrees of freedom. In cold atoms, elastic binary collisions are described by contact interactions proportional to their respective s-wave scattering lengths. For atoms with internal degrees of freedom, their collision interactions generally contain spin dependence, as in spinor atom condensates [19], where the spin-dependent interactions determine the various ground state phases: ferromagnetic or polar for the case of spin-1; ferromagnetic, polar, or cyclic, for spin-2; *etc.* The inclusion of SO coupling induces competition with spin-dependent interactions in addition to modify the single particle spectra for a spinor BEC. As a result, spin-dependent interaction will in turn

influence atomic spatial motion, leading to a variety of density patterns even in the ground state [13–16].

Spontaneously formed patterns in spinor component densities, are essentially spin textures, previously studied in <sup>3</sup>He superfluids and more recently in spinor condensates for both ferromagnetic and anti-ferromagnetic (polar) phases, especially with long-range dipolar interactions [20–26]. Periodically ordered patterns can also arise in superfluids with roton-like spectra [23, 24].

This study addresses ground state pattern formations due to the competition between SO coupling and spin-dependent interactions. The simplest case concerns a spin-1/2 BEC with SO coupling, [13–15], already observed in recent experiments [16]. Depending on the sign of the effective spin interaction strength, which is proportional to the difference between intra- and inter-species atomic scattering strengths, the ground state patterns are found to be either planar or standing waves [13–16]. The same conclusion was reached in recent theoretical studies for a spin-1 BEC [13], where the two ground state phases are ferromagnetic and polar in the absence of SO coupling. Spin-2 condensates, on the other hand, can potentially be very different due to the presence of a cyclic phase when SO coupling is absent. Understanding the associated patterns in a spin-2 BEC thus constitutes an importance objective for new physics in atomic quantum gases with gauge fields.

## II. OUR MODEL

We start by describing our model of a spin-2 BEC [27, 28] in a quasi-two dimensional optical trap  $V_o = m\omega^2(x^2 + y^2 + \lambda^2 z^2)/2$  with  $\lambda \gg 1$ , including SO coupling. The effective Hamiltonian takes the form

$$\begin{aligned} \hat{H} = & \int d\boldsymbol{\rho} \hat{\psi}_i^\dagger \left( \frac{\mathbf{p}^2}{2m} + v_x p_x F_x + v_y p_y F_y + V_o \right)_{ij} \hat{\psi}_j \\ & + \frac{1}{2} \int d\boldsymbol{\rho} \left\{ \alpha' \hat{\psi}_i^\dagger \hat{\psi}_j^\dagger \hat{\psi}_j \hat{\psi}_i + \beta' \hat{\psi}_i^\dagger \hat{\psi}_k^\dagger \mathbf{F}_{ij} \cdot \mathbf{F}_{kl} \hat{\psi}_l \hat{\psi}_j \right. \\ & \left. + \gamma' (-1)^{i+j} \hat{\psi}_i^\dagger \hat{\psi}_{-i}^\dagger \hat{\psi}_j \hat{\psi}_{-j} \right\}, \end{aligned} \quad (1)$$

where  $(F_\mu)_{ij}$  ( $\mu = x, y, z$ ) are the  $(i, j)$  components of spin-2 matrices  $F_\mu$ ,  $V'_o = m\omega^2(x^2 + y^2)/2$ ,  $\alpha'$ ,  $\beta'$  and  $\gamma'$  are reduced two-dimensional effective density-density, spin-exchange, and spin singlet-pairing interaction parameters, respectively.  $v_x$  and  $v_y$  parameterizes the strength of SO coupling. This form of two- and three-component of condensates with SO coupling can be realized with a tripod and a tetrapod plane-wave laser beams setup [7], respectively. Also, recently Y. -J. Lin *et al.* [16] have realized a mixed form of Rashba and Dresselhaus type SO coupling interaction for pseudo spin-1/2 system. They further suggested that we can realize the SO coupled spin-1 or spin-2 condensates by using a smaller quadratic Zeeman shift.

The single particle Hamiltonian

$$\hat{H}_0 = \frac{\mathbf{p}^2}{2m} + v_x p_x F_x + v_y p_y F_y, \quad (2)$$

ignoring the external trapping potential, can be easily diagonalized using plane wave basis, leading to eigenvalues  $E_\lambda(\mathbf{p})$  and eigenvectors  $\phi_\lambda(\mathbf{k}) = e^{i\mathbf{k}\cdot\rho}\zeta_\lambda(\mathbf{k})$  given by

$$\begin{aligned} E_\lambda(\mathbf{k}) &= \frac{\hbar^2 \mathbf{k}^2}{2m} + \lambda \sqrt{\hbar^2 v_x^2 k_x^2 + \hbar^2 v_y^2 k_y^2}, \quad (3) \\ \zeta_2^T(\mathbf{k}) &= (\chi_{\mathbf{k}}^{*2}, 2\chi_{\mathbf{k}}^*, \sqrt{6}, 2\chi_{\mathbf{k}}, \chi_{\mathbf{k}}^2)/4, \\ \zeta_1^T(\mathbf{k}) &= (-\chi_{\mathbf{k}}^{*2}, -\chi_{\mathbf{k}}^*, 0, \chi_{\mathbf{k}}, \chi_{\mathbf{k}}^2)/2, \\ \zeta_0^T(\mathbf{k}) &= (\sqrt{3}\chi_{\mathbf{k}}^{*2}, 0, -\sqrt{2}, 0, \sqrt{3}\chi_{\mathbf{k}}^2)/2\sqrt{2}, \\ \zeta_{-1}^T(\mathbf{k}) &= (-\chi_{\mathbf{k}}^{*2}, \chi_{\mathbf{k}}^*, 0, -\chi_{\mathbf{k}}, \chi_{\mathbf{k}}^2)/2, \\ \zeta_{-2}^T(\mathbf{k}) &= (\chi_{\mathbf{k}}^{*2}, -2\chi_{\mathbf{k}}^*, \sqrt{6}, -2\chi_{\mathbf{k}}, \chi_{\mathbf{k}}^2)/4. \quad (4) \end{aligned}$$

In the above  $\lambda = \pm 2, \pm 1, 0$  labels the respective energy band and  $\chi_{\mathbf{k}} = (v_x k_x + i v_y k_y) / \sqrt{v_x^2 k_x^2 + v_y^2 k_y^2}$ . Corresponding to the above eigenvectors Eq. (4), we find the two order parameters ( $|\langle \mathbf{F} \rangle| = |\zeta_\lambda^\dagger \mathbf{F} \zeta_\lambda|$  and  $|\langle \Theta \rangle| = |(-)^j \zeta_{\lambda, j} \zeta_{\lambda, -j}|$ ) are equal to  $(2, 0)$ ,  $(1, 0)$ , and  $(0, 1)$  corresponding to  $\lambda = \pm 2, \pm 1, 0$ , respectively.

The ground state of the single particle Hamiltonian (2):  $\phi_{-2}(\mathbf{k}_g)$ , is two-fold degenerate for  $|v_x| \neq |v_y|$ ; and is infinitely degenerate if  $|v_x| = |v_y|$ . For the former case,  $\hbar \mathbf{k}_g = (\pm 2m|v_x|, 0)$  if  $|v_x| > |v_y|$ , while  $\hbar \mathbf{k}_g = 2m|v_x|(\cos \theta_g, \sin \theta_g)$  for any  $\theta_g \in [0, 2\pi)$ , in the latter case with  $|v_x| = |v_y|$ . Atomic spins are fully polarized with  $|\langle F \rangle| = 2$  for both cases.

### III. GROUND-STATE PATTERNS

When SO coupling is absent, the ground states for a spin-2 BEC including collision interactions, takes three phases: ferromagnetic, polar, and cyclic [27, 28]. Their corresponding spin-dependent interactions will in this study be called “ferromagnetic”, “polar”, and “cyclic” interactions. In the presence of SO coupling, we discuss their possible ground states for the above three types of spin-dependent interactions. The external trapping potential is neglected in analytical treatments, while

it is weakened appreciably for numerical studies with imaginary-time propagation of coupled Gross-Pitaevskii equations (GPEs). Including axisymmetric SO interaction, the ground states can be approximately understood by applying perturbation theory to the degenerate single particle states. Each of the three types of spin-dependent interactions is found to be associated with a distinct number single-particle states. For the case of “cyclic” interaction, this approximation breaks with increasing asymmetry of SO coupling.

(A) “Ferromagnetic” interaction The ferromagnetic spin-exchange interaction tends to polarize atoms’ spin, consistent with the ground state of the single-particle Hamiltonian. As a result, all atoms condense into any single particle ground state  $\phi_{-2}(\mathbf{k}_g)$ . The spin rotation and time-reversal symmetry are broken in this case. The optical trap and the spin-independent interactions will change atomic density distributions slightly.

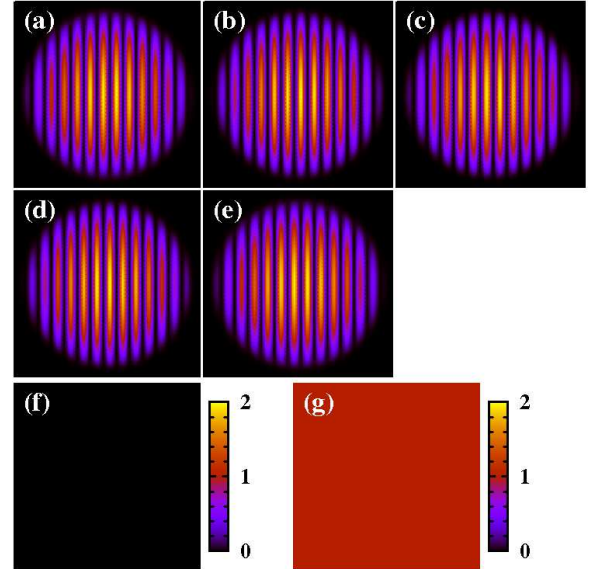


FIG. 1: (Color online). Ground states of a spin-2 BEC in the “polar” interaction case with SO coupling for  $v_x = 2v_y$  and  $\gamma' = -\beta' = -0.2\alpha' < 0$ . (a-e) Density distributions for the five spin components:  $M_F = +2, +1, 0, -1, -2$ . Yellow and black colors represent high and low density respectively. (f-g) Spatial distributions of two order parameters (uniform in this case)  $|\langle \mathbf{F} \rangle|$  and  $|\langle \Theta \rangle|$ , which approximately measure spin-exchange and singlet-pairing interactions, respectively.

(B) “Polar” interaction The order parameter  $|\langle F \rangle| = 2$  in the single particle ground state conflicts with the polar phase of  $|\langle F \rangle| = 0$ . A superposition of degenerate single particle states is adopted

$$\psi = \sum_{\mathbf{k}_g} C_g \phi_{-2}(\mathbf{k}_g), \quad (5)$$

to minimize the spin-dependent interaction. The states  $\phi_{-2}(\mathbf{k}_g)$  are orthogonal, thus the superposition state  $|\psi\rangle$  does not affect kinetic energy. The suitable coefficients  $C_g$  should give  $|\langle \psi | \mathbf{F} | \psi \rangle| = 0$  and  $|\langle \psi | \Theta | \psi \rangle| = 1$ ,

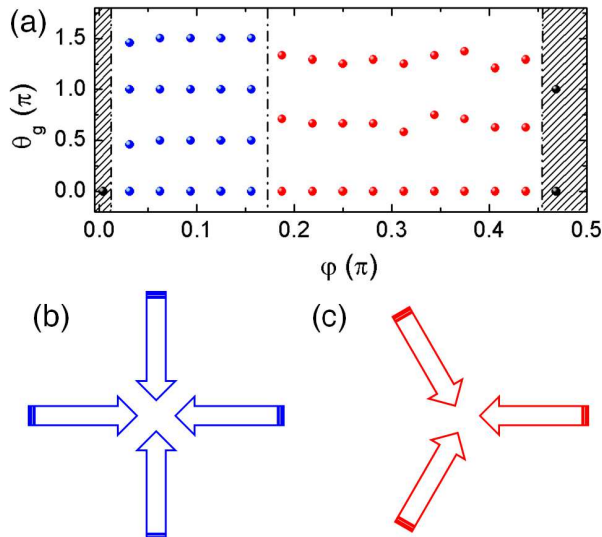


FIG. 2: (Color online). Ground states of a spin-2 BEC in the “cyclic” interaction case with SO coupling for  $v_x = v_y$ . (a) The number of plane waves in the ground states with changing  $\varphi = \arg(\gamma' + i\beta')$ . The column of 4 blue (3 red) dots denote four (three) plane waves. The shadow window with one or two black dots denote one or two plane waves respectively constituting of the ground states. Schematic illustrations of four b) [three c)] plane wave superpositions responsible for square (triangular) density modulations. The angles between the directions of two nearby plane waves are close but not exactly equal to  $2\pi/4$  or  $2\pi/3$  due to frustration.

while preserving the spin-independent interaction energy. It is easy to conclude a superposition of two counter-propagating single particle states meets this criterion, thus the ground state is given by  $\phi_{-2}(\mathbf{k}_g) + e^{i\vartheta}\phi_{-2}(-\mathbf{k}_g)$ , where the time-reversal symmetry remains valid. Back into the  $z$ -axis quantized representation, the interference between the two counter-propagating plane waves induce density oscillations in spinor components. In the quantization direction of  $\mathbf{k}_g$ , however, only  $M_F = \pm 2$  components are found to be populated, each with smooth density, respectively propagating into opposite directions.

In Figure 1, we illustrate density distributions of the spin components and the spatial dependence of two order parameters  $|\langle \mathbf{F} \rangle|$  and  $|\langle \Theta \rangle|$  for  $v_x = 2v_y$  and  $\gamma' = -\beta' = -0.2\alpha' < 0$ . When  $|v_x| > |v_y|$  ( $|v_x| < |v_y|$ ), we find the plane waves propagate along the positive/minus  $x$ -axis ( $y$ -axis) the ground state, resulting in density modulations along  $x$ -axis ( $y$ -axis). Figure 1(f-g) shows the two order parameters are uniformly distributed, with  $|\langle \mathbf{F} \rangle| = 0$  and  $|\langle \Theta \rangle| = 1$ , consistent with previous discussions. A cautionary note concerns the axis-symmetric case of  $|v_x| = |v_y|$ . Due to the spin-independent interaction, the ground state consists of only one pair of counter-propagating plane waves, although superpositions of two or more counter-propagating pairs also minimize spin-dependent energy.

(C) “Cyclic” interaction First, we consider the sym-

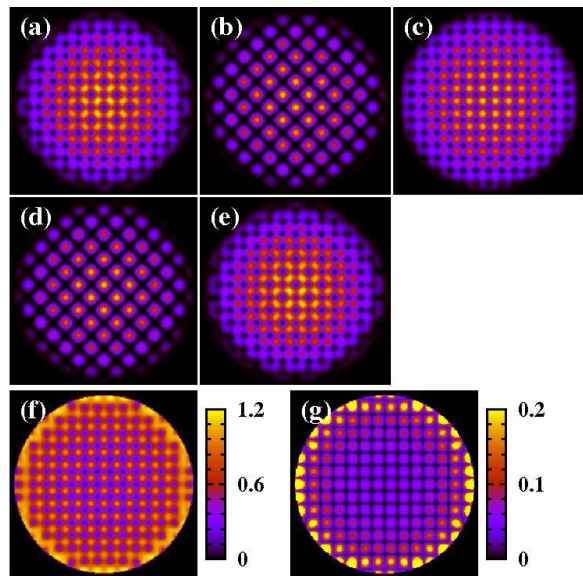


FIG. 3: (Color online). Ground states of a spin-2 BEC in the “cyclic” interaction case with SO coupling for  $v_x = v_y$ ,  $\gamma' = 0.2\alpha'$ , and  $\beta' = 0.02\alpha'$ . (a-e) Density distributions of the spin components:  $M_F = +2, +1, 0, -1, -2$ . Yellow and black colors represent high and low densities respectively. (f-g) Spatial distributions of the order parameters  $|\langle \mathbf{F} \rangle|$  and  $|\langle \Theta \rangle|$ , reflecting spin-exchange and singlet-pairing interactions respectively.

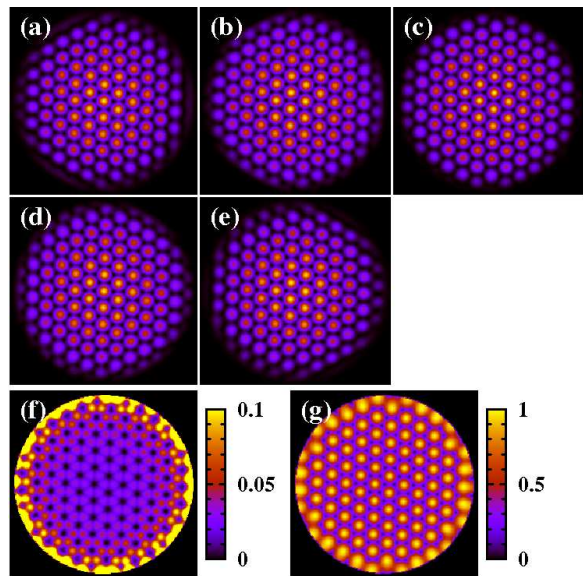


FIG. 4: (Color online). The same as in Fig. 3 but for  $v_x = v_y$ ,  $\gamma' = 0.02\alpha'$  and  $\beta' = 0.2\alpha'$ .

metric case of  $|v_x| = |v_y|$ . As pointed out in the above “polar” interaction case, superpositions of single particle ground states are tried to minimize the interaction energy. Numerically, the minimization procedure is achieved with simulated annealing. In Fig. 2(a), the ground states are found to contain several plane

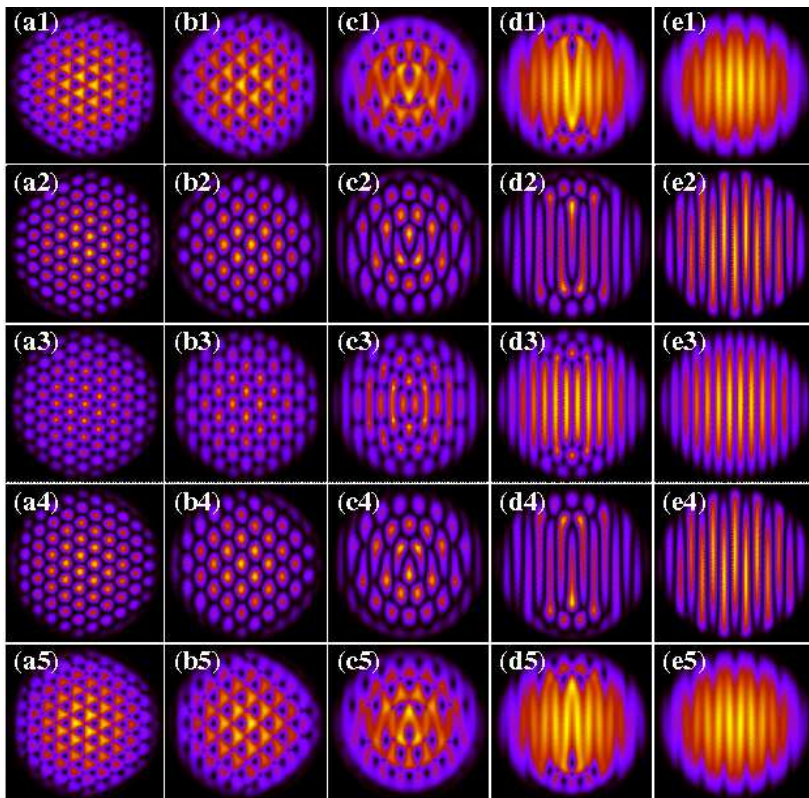


FIG. 5: (Color online). Ground states of a spin-2 BEC in the “cyclic” interaction case with SO coupling for  $\gamma' = \beta' = 0.2\alpha'$ . (a1-a5) Spinor component densities at  $v_y = v_x$ , from up to down corresponding to  $M_F = +2, +1, 0, 1, 2$ . (b1-b5), (c1-c5), (d1-d5), and (e1-e5) are as in (a1-a5) but for  $v_y = 3v_x/4$ ,  $v_y = 17v_x/24$ ,  $v_y = 2v_x/3$ , and  $v_y = v_x/2$ , respectively.

waves with significant weights if they are assumed approximately to consist of a series of degenerate single particle ground states with momentum  $\hbar\mathbf{k}_g = 2m|v_x|(\cos\theta_g, \sin\theta_g)$  and if external optical trapping potentials are neglected. In this case, the spin-dependent interactions couple degenerate single particle ground states, and result in discrete rotation symmetry of the ground states. Starting from the boundary of  $\beta' = 0$ , with increasing value of  $\varphi = \arg(\gamma' + i\beta')$ , the ground states at first contains only one plan wave, as  $\varphi$  exceeds a small critical value determined by the three interaction parameters, the ground states display periodic square lattices in the spin component densities. Further increasing of  $\varphi$  arrives at the critical value  $\varphi_c$ , where the ground states change into triangular from superpositions of three plane waves until near the boundary with  $\gamma' = 0$ , where the ground state superpositions reduce to contain two counter-propagating plan waves. It is important to emphasize that interference between several plane waves may increase density-density interaction energy, which explains why the phase boundaries between the ground states with four and one, also with three and two plan waves, deviate from  $\varphi = 0$  or  $\varphi = \pi/2$ . The numerical results show for the two different types of ground states with square or triangular patterns, the angles between nearby plane waves are close to but not exactly equal to  $2\pi/4$  or  $2\pi/3$  respectively, and the nonzero coefficients  $C_g$  are not all exactly equal, although they are of the same orders of magnitudes.

To validate our proposition that the ground states of

a spin-2 BEC with SO interaction are approximate superpositions of degenerate single particle ground states in the absence of the trap potential, we numerically solve the GPEs directly using imaginary-time propagation including the optical trap. Figures 3 and 4 show spin component densities and the spatial dependence of the two order parameters  $|\langle\mathbf{F}\rangle|$  and  $|\langle\Theta\rangle|$  for two different cases. They confirm our understanding that not only spin component density distributions but the two order parameters show square or triangular patterns. More carefully, the shapes of density distributions within each unit cell are not identical for the five spin components at a fixed  $\varphi$ . Their differences vary as  $\varphi$  is changed. Because the values of  $C_g$  are not exactly equal, they generally vary with  $\varphi$  constrained by the spin-independent interaction term, although the number of plane waves contained in the ground states remains at four or three.

Next, we consider the asymmetric case of  $|v_x| \neq |v_y|$ , where the single particle ground states are two-fold degenerate. When insufficient number of degenerate single particle ground states exist to construct square or triangular shaped density distributions, our proposition fails. This is also validated by numerical simulations. In Fig. 5, we illustrate results from numerical simulations. From (a1-a5), (b1-b5), (c1-c5), (d1-d5), to (e1-e5), the asymmetry of the SO coupling is increased, realized by fixing  $v_x$  while decreasing  $v_y$  from being equal  $v_x$ ,  $3v_x/4$ ,  $17v_x/24$ ,  $2v_x/3$  to  $v_x/2$ , respectively. The ground state show triangular density distributions in each component at  $v_y = v_x$ . The triangular lattice is deformed into al-

most square lattice distributions when  $v_y$  is decreased into  $3v_x/4$ , and gradually evolve in the end into striped patterns reflecting the underline two-fold degeneracy as we further decrease  $v_y$ .

#### IV. CONCLUSION

In conclusion, we study spin-2 condensates with SO coupling. Due to the competition among SO coupling, spin-dependent, and spin-independent interactions, the ground states are found to contain one or two counter-propagating plane waves respectively in “ferromagnetic” and “polar” interaction cases, where both the single particle Hamiltonian and atomic interaction energies can reach their corresponding minimum values. For “cyclic” interaction case with axisymmetric SO coupling, the ground states can be categorized into two different types respectively containing four or three plane waves, leading to square or triangular patterns correspondingly. For

asymmetric SO coupling, the ground states are determined by the ratio of two SO coefficients:  $|v_y|/|v_x|$ . As long as ratio is decreased, the spin component density distributions can evolve from triangular to square shaped lattices before asymptotically reaching the striped pattern. This structure phase transition provides a clear signature for SO coupling. In the “cyclic” interaction case, the corresponding minimum value of single particle Hamiltonian and the interaction energies cannot be reached simultaneously.

#### V. ACKNOWLEDGMENTS

Z.F.X thanks Masahito Ueda for valuable discussions. This work is supported by NSF of China under Grants No. 11004116 and No. 10974112, NKBRF of China, and the research program 2010THZO of Tsinghua University.

- 
- [1] Alexander L. Fetter, *Rev. Mod. Phys.* **81**, 647 (2009).
  - [2] N. R. Cooper, *Adv. Phys.* **57**, 539 (2008).
  - [3] Jean Dalibard, Fabrice Gerbier, Gediminas Juzeliūnas, and Patrik Öhberg, arXiv: 1008.5378.
  - [4] G. Juzeliūnas, P. Öhberg, J. Ruseckas, and A. Klein, *Phys. Rev. A* **71**, 053614 (2005); G. Juzeliūnas, J. Ruseckas, P. Öhberg, and M. Fleischhauer, *Phys. Rev. A* **73**, 025602 (2006).
  - [5] Kenneth J. Günter, Marc Cheneau, Tarik Yefsah, Steffen P. Rath, and Jean Dalibard, *Phys. Rev. A* **79**, 011604 (2009)
  - [6] Y.-J. Lin, R. L. Compton, A. R. Perry, W. D. Phillips, J. V. Porto and I. B. Spielman, *Phys. Rev. Lett.* **102**, 130401 (2009); Y.-J. Lin, R. L. Compton, K. Jimenez-Garcia, J.V. Porto, and I. B. Spielman, *Nature (London)* **462**, 628 (2009).
  - [7] J. Ruseckas, G. Juzeliūnas, P. Öhberg, and M. Fleischhauer, *Phys. Rev. Lett.* **95**, 010404 (2005); Gediminas Juzeliūnas, Julius Ruseckas, and Jean Dalibard *Phys. Rev. A* **81**, 053403 (2010).
  - [8] K. Osterloh, M. Baig, L. Santos, P. Zoller, and M. Lewenstein, *Phys. Rev. Lett.* **95**, 010403 (2005).
  - [9] Indubala I. Satija, Daniel C. Dakin, and Charles W. Clark, *Phys. Rev. Lett.* **97**, 216401 (2006).
  - [10] I. Žutić, J. Fabian, S. Das Sarma, *Rev. Mod. Phys.* **76**, 323 (2004).
  - [11] Janne Ruostekoski, Gerald V. Dunne, and Juha Javanainen, *Phys. Rev. Lett.* **88**, 180401 (2002).
  - [12] Tudor D. Stanescu, Brandon Anderson, and Victor Galitski, *Phys. Rev. A* **78**, 023616 (2008).
  - [13] Chunji Wang, Chao Gao, Chao-Ming Jian, and Hui Zhai, *Phys. Rev. Lett.* **105**, 160403 (2010).
  - [14] Tin-Lun Ho and Shizhong Zhang, arXiv: 1007.0650.
  - [15] S.-K. Yip, arXiv: 1008.2263.
  - [16] Y.-J. Lin, K. Jiménez-García, and I. B. Spielman, *Nature (London)* **471**, 83 (2011).
  - [17] M. Merkl, A. Jacob, F. E. Zimmer, P. Öhberg, and L. Santos, *Phys. Rev. Lett.* **104**, 073603 (2010).
  - [18] Daniel Braun, *Phys. Rev. A* **82**, 013617 (2010).
  - [19] Masahito Ueda and Yuki Kawaguchi, arXiv: 1001.2072.
  - [20] Wenxian Zhang, D. L. Zhou, M.-S. Chang, M. S. Chapman, and L. You, *Phys. Rev. Lett.* **95**, 180403 (2005);
  - [21] L. E. Sadler, J. M. Higbie, S. R. Leslie, M. Vengalattore, D. M. Stamper-Kurn, *Nature* **443**, 312 (2006).
  - [22] Hiroki Saito, Yuki Kawaguchi, and Masahito Ueda, *Phys. Rev. Lett.* **102**, 230403 (2009).
  - [23] R. W. Cherng and E. Demler, *Phys. Rev. Lett.* **103**, 185301 (2009).
  - [24] Michał Matuszewski, *Phys. Rev. Lett.* **105**, 020405 (2010).
  - [25] Jochen Kronjäger, Christoph Becker, Parvis Soltan-Panahi, Kai Bongs, and Klaus Sengstock, *Phys. Rev. Lett.* **105**, 090402 (2010).
  - [26] M. Scherer, B. Lücke, G. Gebreyesus, O. Topic, F. Deuretzbacher, W. Ertmer, L. Santos, J. J. Arlt, and C. Klempt, *Phys. Rev. Lett.* **105**, 135302 (2010).
  - [27] C. V. Ciobanu, S.-K. Yip, and Tin-Lun Ho, *Phys. Rev. A* **61**, 033607 (2000).
  - [28] Masato Koashi and Masahito Ueda, *Phys. Rev. Lett.* **84**, 1066 (2000).